

Status of radiation effects of the ATLAS SCT detector

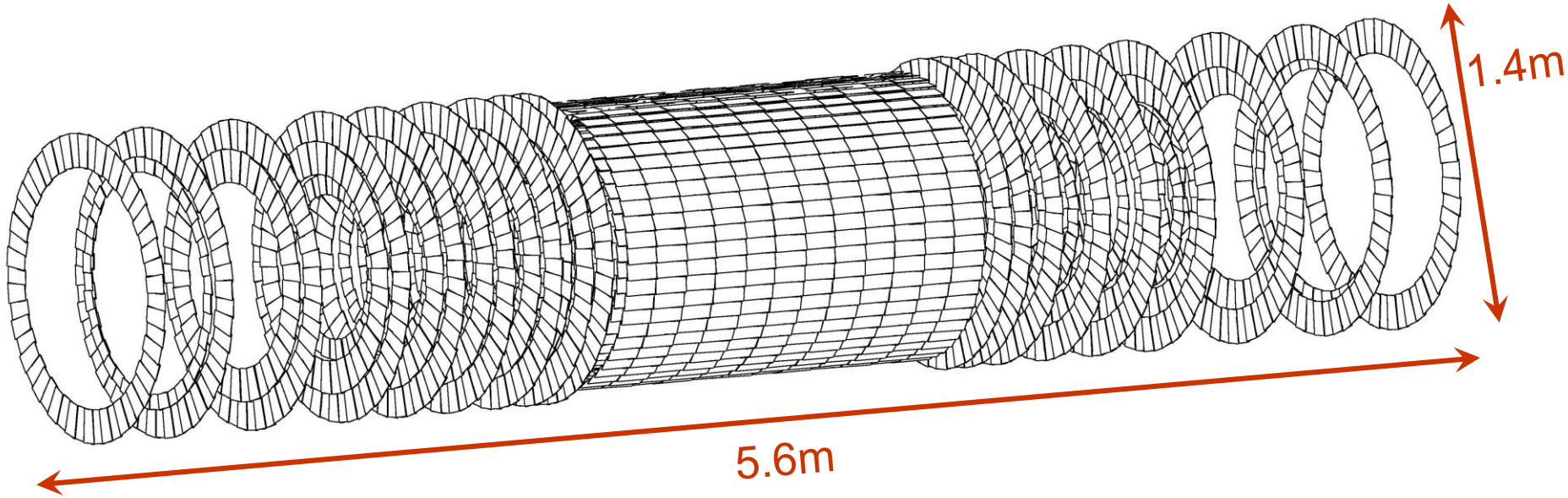
22nd RD50 Workshop on Radiation Hard Semiconductor Devices
for Very High Luminosity Colliders

at University of New Mexico, Albuquerque, USA

June 3, 2013

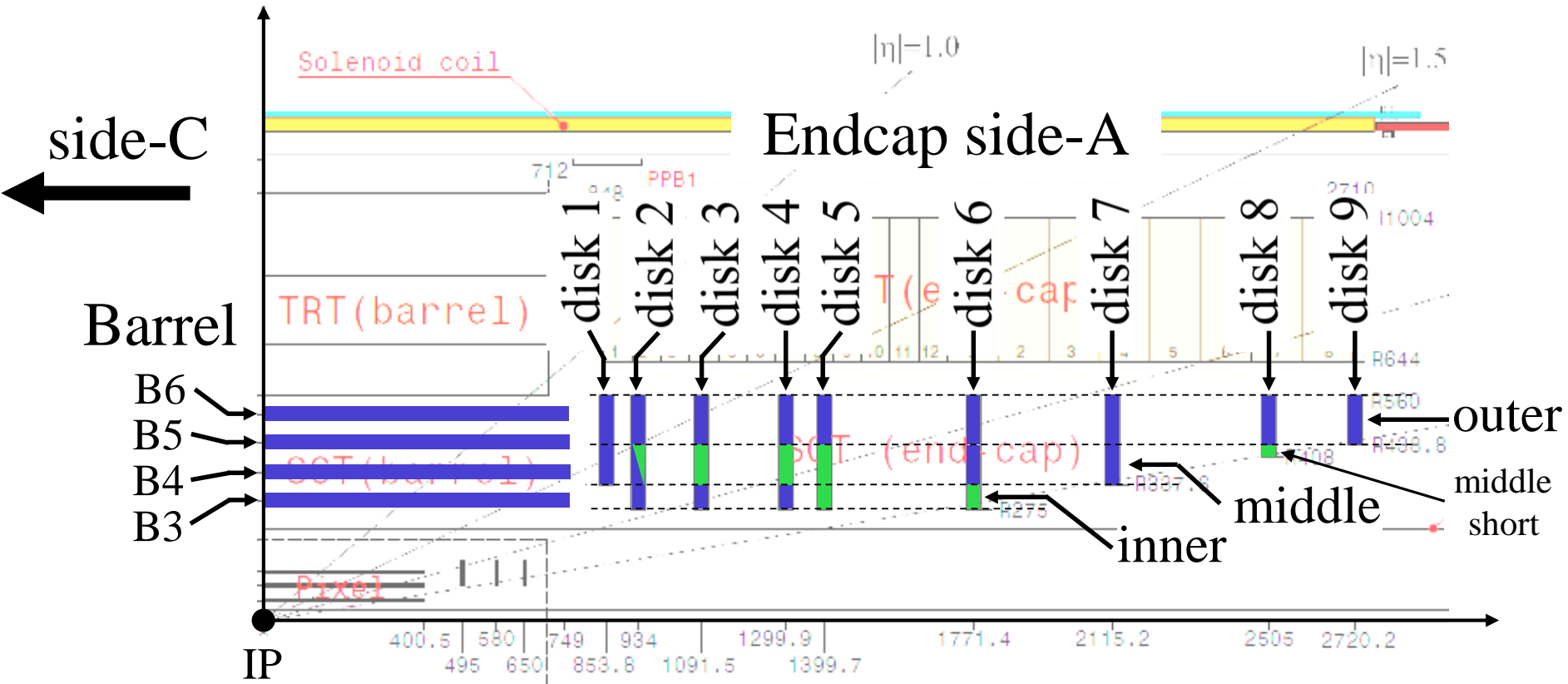
Taka Kondo (KEK)
on behalf of the ATLAS SCT Collaboration

The Semi Conductor Tracker (SCT)



- 61 m² of silicon with 6.3 million readout channels
- 4088 silicon modules in 4 Barrels and 18 EC Disks
- C₃F₈ Cooling (-7°C to +6°C silicon)

SCT module layout and appellation



■ modules with **Hamamatsu** sensors

■ modules with **CiS** sensors

SCT Sensors [1]

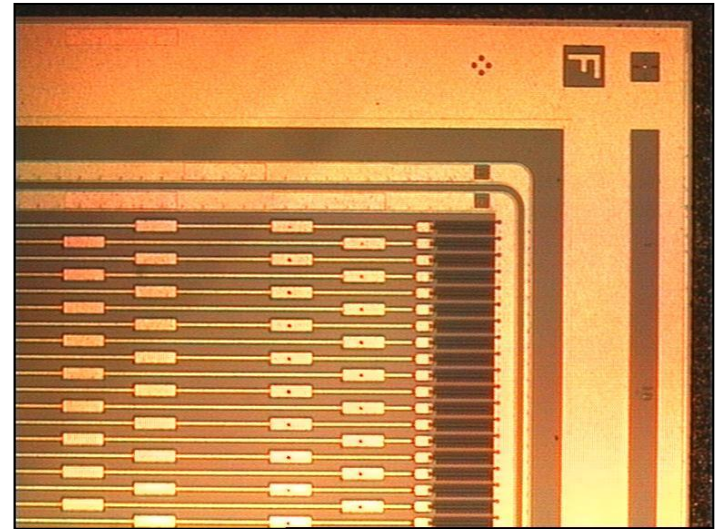
- Single sided p-on-n
- 285 μm thick
- 768+2 AC-coupled strips

Barrel

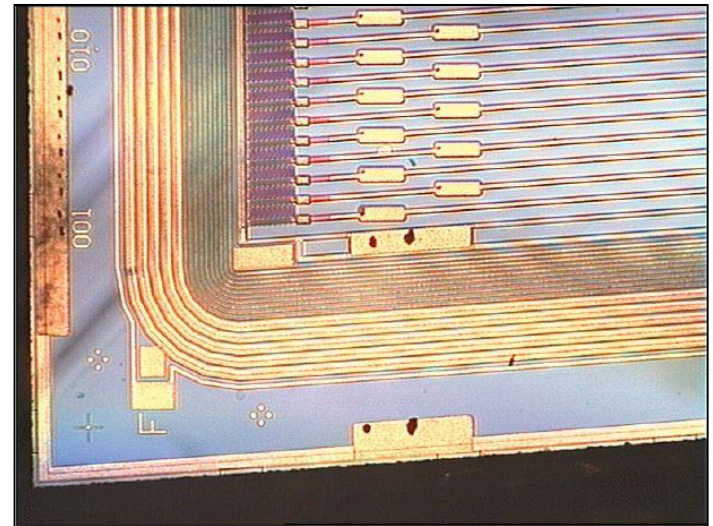
- 8448 barrel sensors
- 8081 sensors with $\langle 111 \rangle$
- 367 (4.4%) sensors with $\langle 100 \rangle$
mounted on B3, B5 and B6
- 64.0 x 63.6 mm²
- 80 μm strip pitch
- 100% Hamamatsu

Endcap

- 6944 wedge sensors
- 56.9-90.4 μm strip pitch
- 5 different shapes
- 74.9% Hamamatsu $\langle 111 \rangle$
- 17.1% CiS $\langle 111 \rangle$
- 8.0% CiS oxygen-enriched $\langle 111 \rangle$



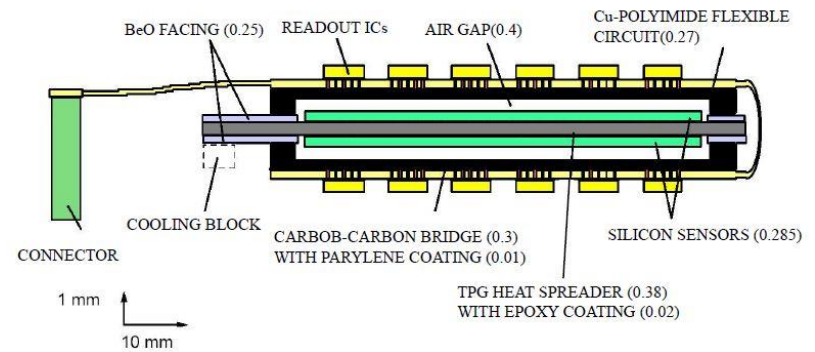
Barrel sensors (Hamamatsu)



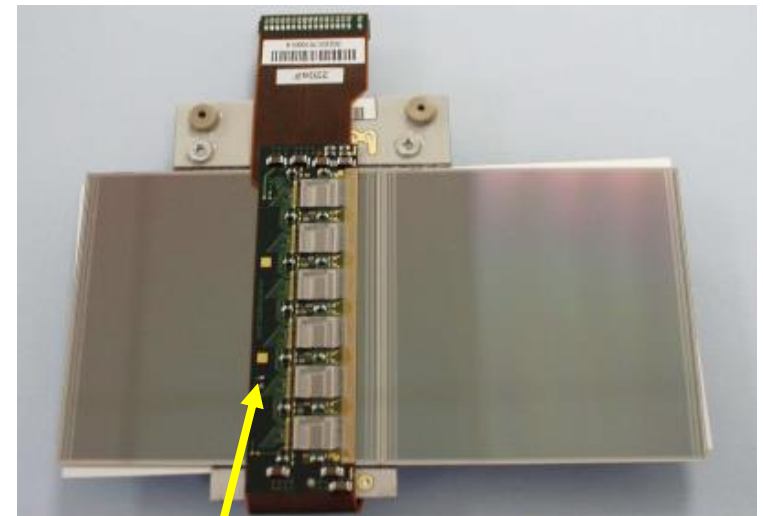
Endcap sensors (CiS)

SCT Modules [1,2]

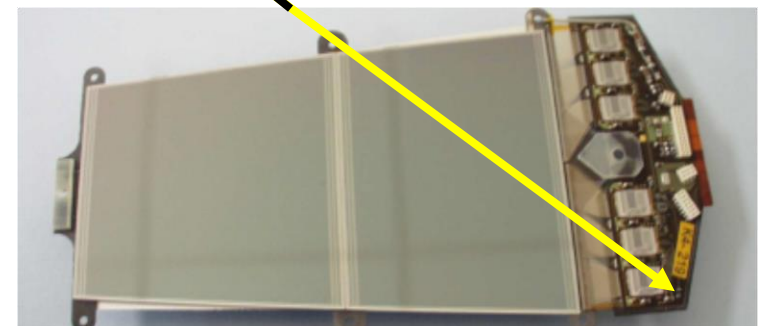
- 2 sensors connected by wire bonding to form 12cm long strips.
- 4 sensors / module
- Glued back to back with $< 8\mu\text{m}$ accuracy between two planes.
- Stereo angle 40 mrad.
- Thermal pyrolytic graphite (TPG) heat spreaders for good thermal conduction and mechanical strength.
- Cu-Polyimide flexible circuits.
- 12 bi-CMOS binary readout chips (128ch) with 1fC threshold [3].
- Power: 6W (chips) + 2W (sensors).
- Radiation length $1.17\%X_0$ (barrel).



Xsection of barrel module

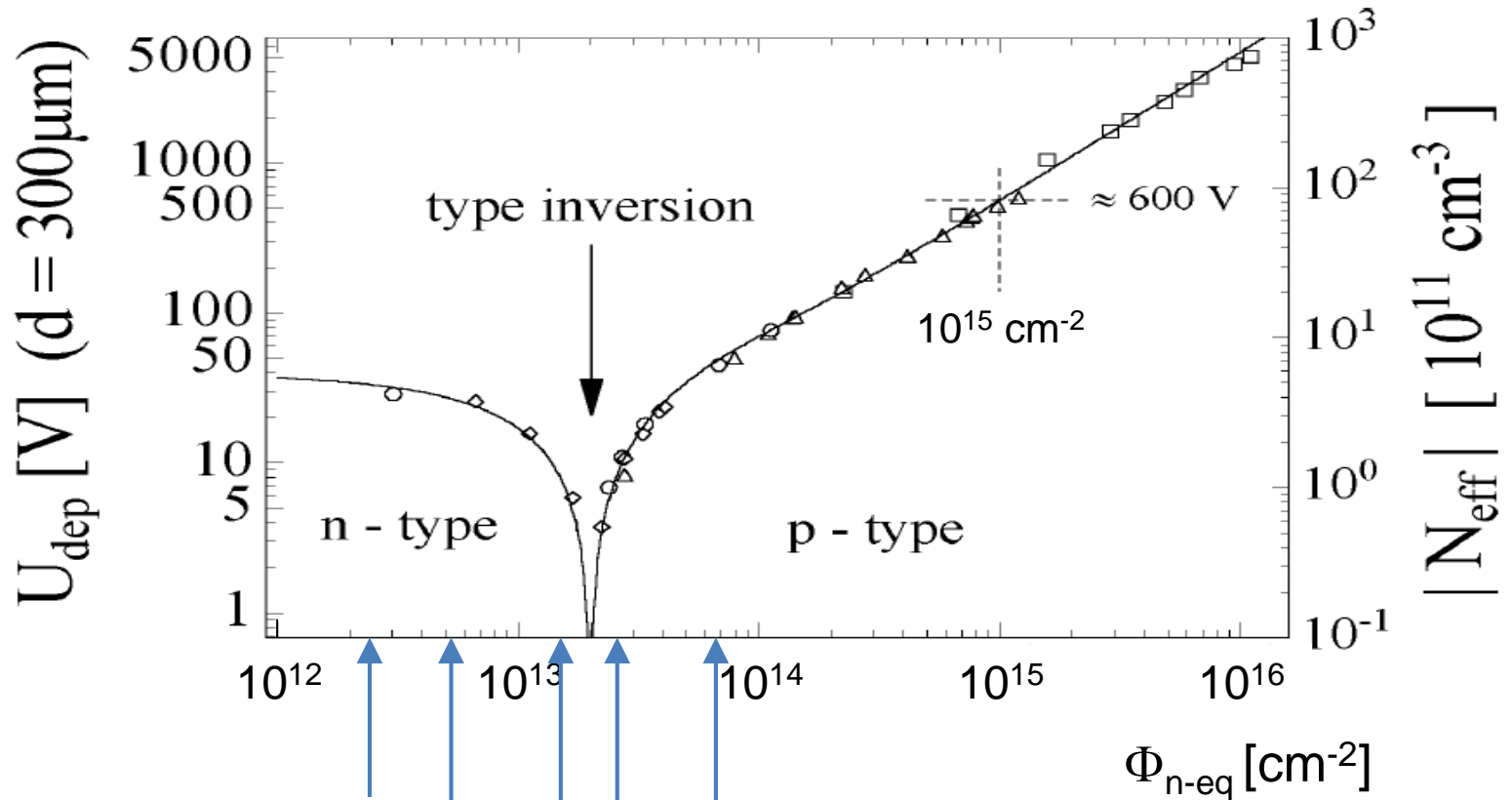


Thermistors for temperature meas.



[1] A. Abdesselam et al., NIM A 568 (2006) 642.
 [2] A. Abdesselam et al., NIM A 575 (2007) 353.
 [3] F. Campabadal, et al., NIM A 552 (2005) 292.

Estimated radiation level by the end of 2012



**1 MeV n-eq fluence
received**

**Integrated luminosity delivered =
5.8 (7 TeV) + 23.8 (8 TeV) fb^{-1}
+ using the Fluka simulation**

[1] Figure copied from p.111 of M. Moll's PhD Thesis (1999).

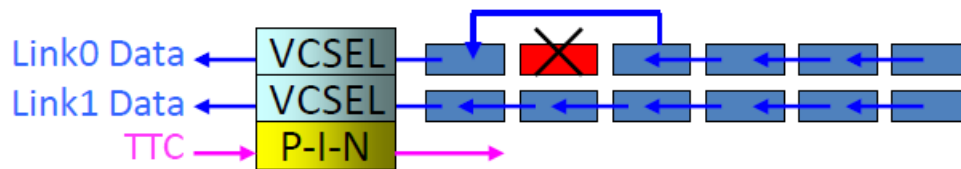
SCT operation and performance

- Keeping low percentage of defect chips/modules (as of Feb 2013).

components	Total	defect components			
		Barrel	Endcap	SCT	Fraction(%)
modules	4088	11	19*	30	0.73 %
chips	49056	38	11	49	0.10 %
strips	6279168	4111	8020	12131	0.21 %

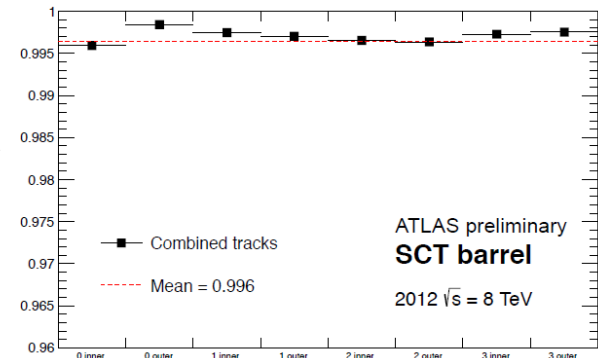
* 13 due to one cooling loop failure

mainly thanks to the built-in **redundancy**.



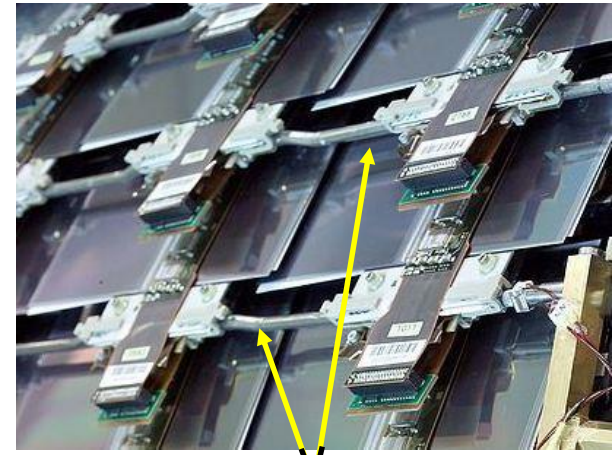
Dead chip bypassed
All fibres ok

- High efficiency for charged particles:
> 99.5% at 8 TeV
- Stop-less recovery for ROD busy cases.
- Periodical auto-configuration of modules to cope with noticeable single event upsets (SEU).

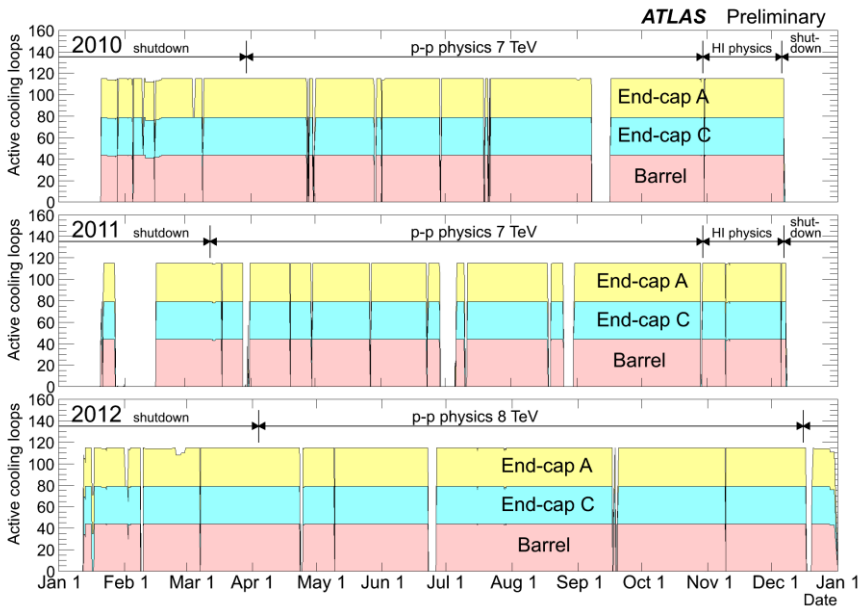


SCT module cooling [1]

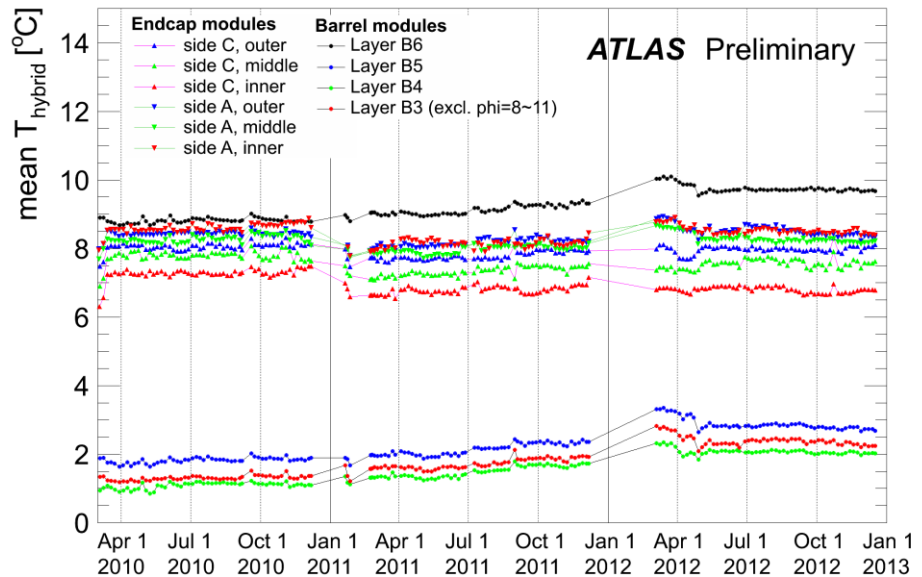
- C_3F_8 evaporative system.
- Very stable operation except initial-stage compressor problems.
- To be replaced with thermo-siphon scheme during 2013/14 shutdown.



Cooling pipes



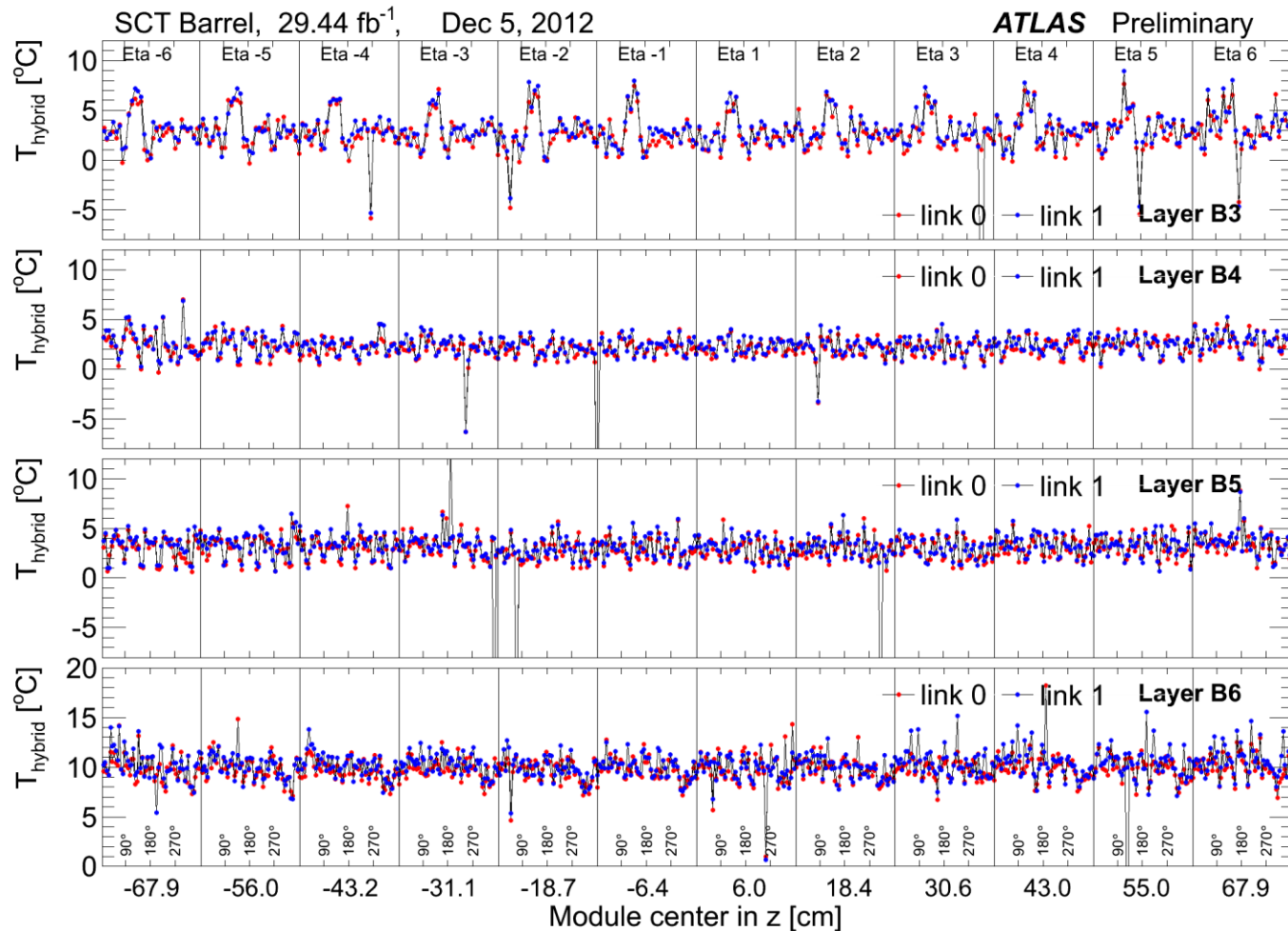
Number of active cooling loops from 2010 to the end of 2012.



Average hybrid temperature of all barrel layers and endcap disks.

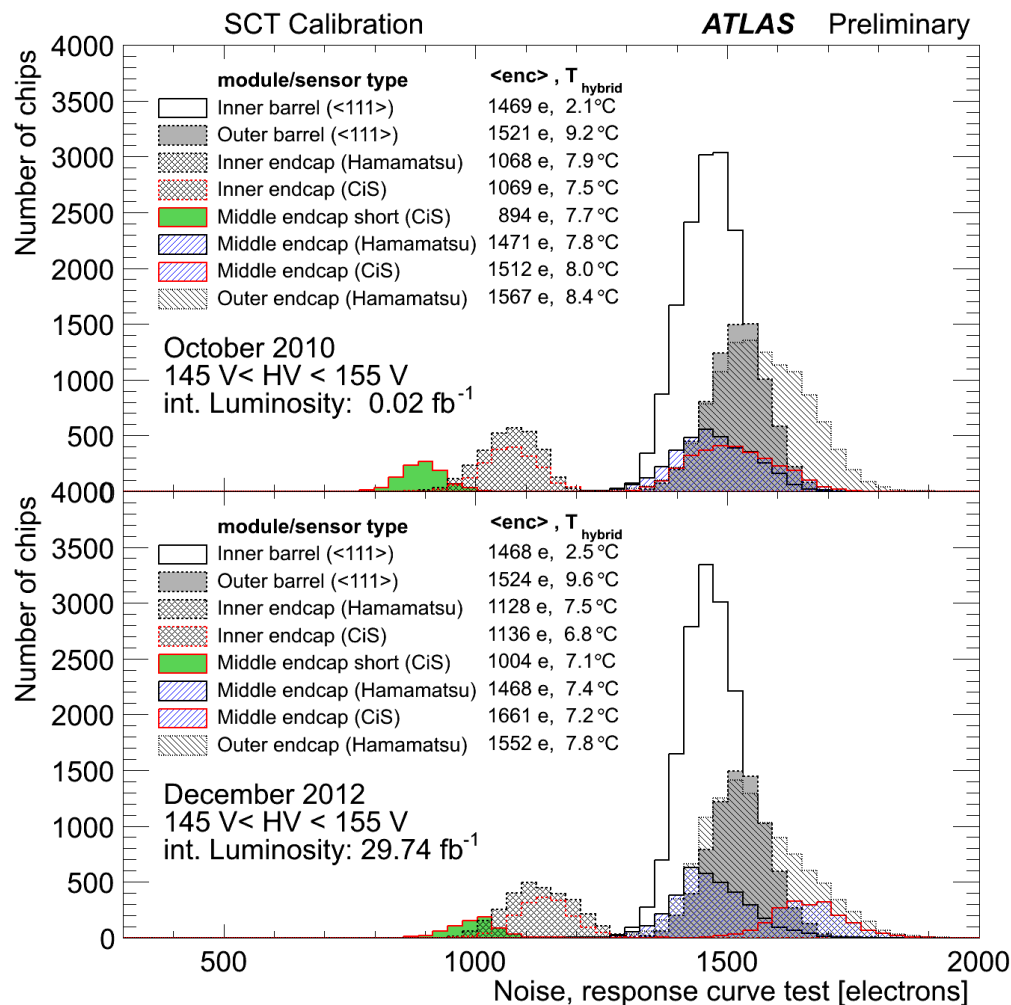
[1] D. Attree et al., 2008 JINST 3 P07003.

Distribution of hybrid Temperature: each module



- (1) Very uniform in ϕ and z directions.
- (2) Bumps in layer B3 is due to one cooling loop set at higher value initially.
- (3) Sensor temperature = hybrid temperature - 3.7°C (FEM results).

Distribution of chip averaged Noise (response curve)

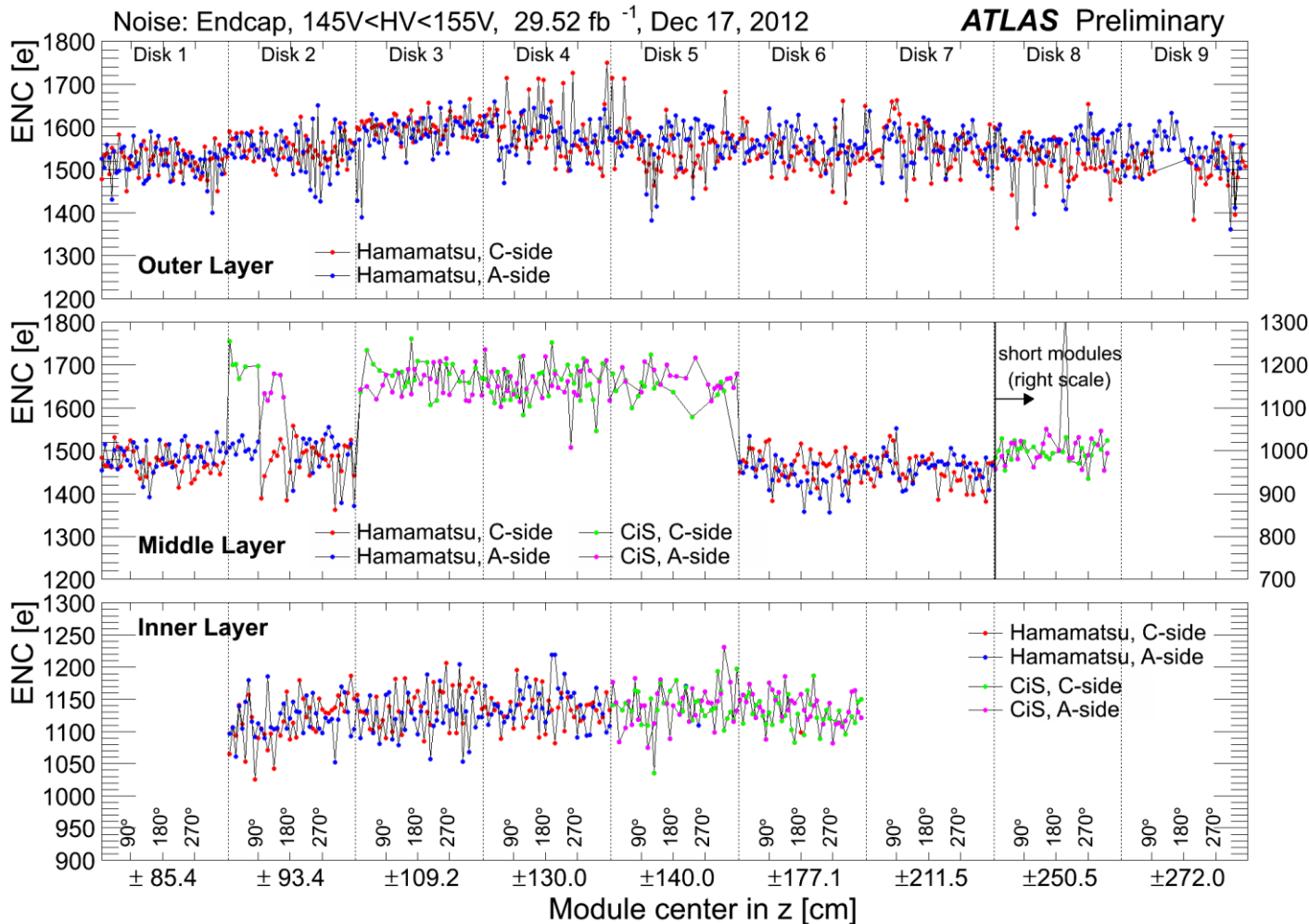


Oct. 2010

Dec. 2012

- (1) Noise (response curve) is deduced from the width of threshold curves at 2 fC charge injection in the gain calibration runs.
- (2) Middle CiS modules show ~10% increase from 2101 to 2012.

Noise of each module: endcap case, Dec. 2012

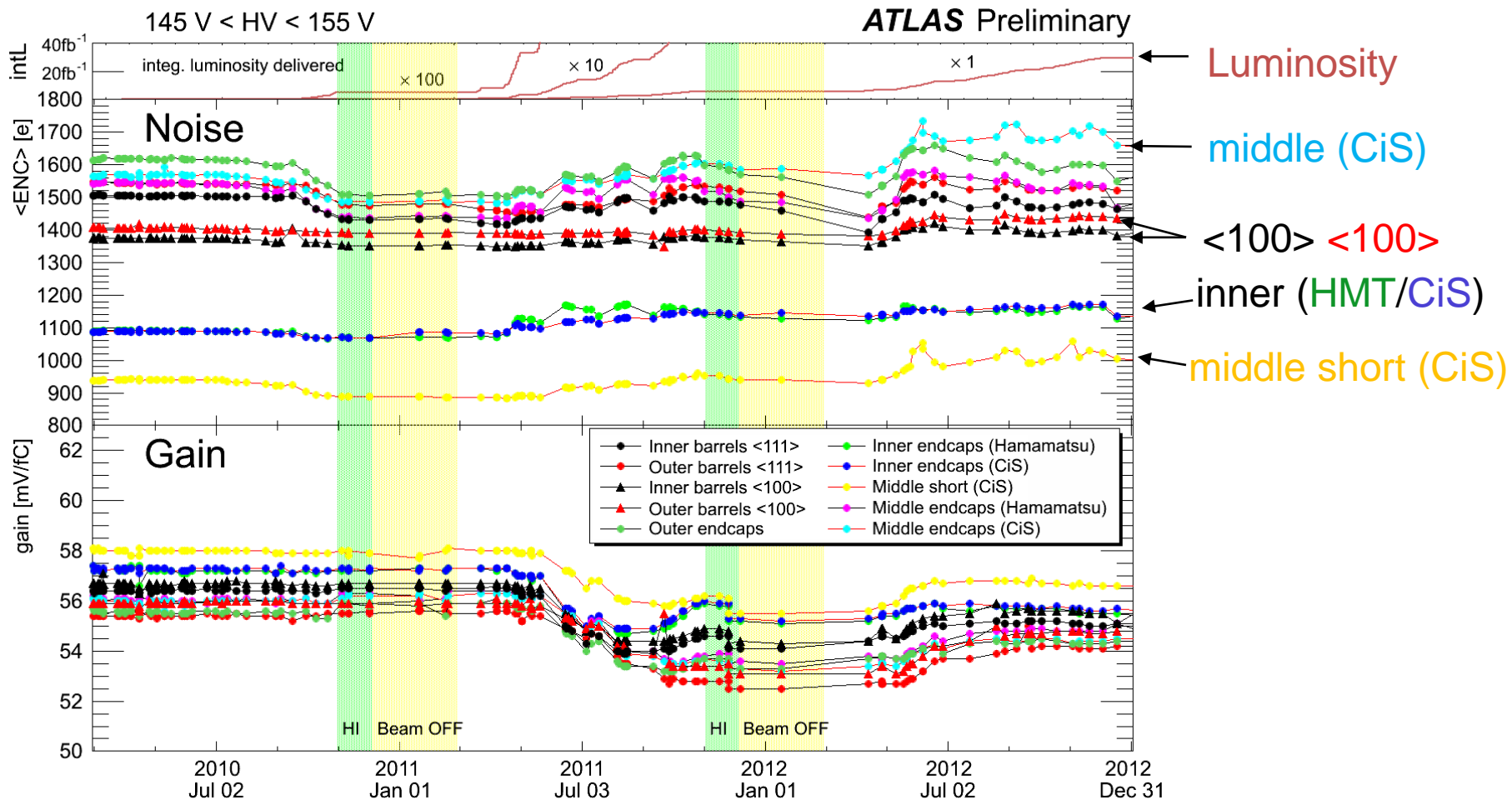


Hamamatsu
 red: C-side
 blue: A-side

CiS
 green: C-side
 pink: A-side

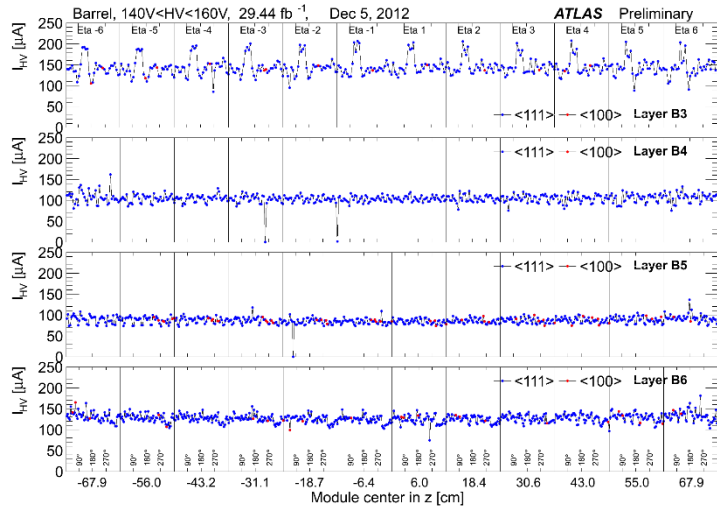
- (1) Middle CiS modules (green, pink) show excess noise.
- (2) Inner CiS modules (oxygen-enriched) stay comparable with others.

Stability of Noise and chip Gain

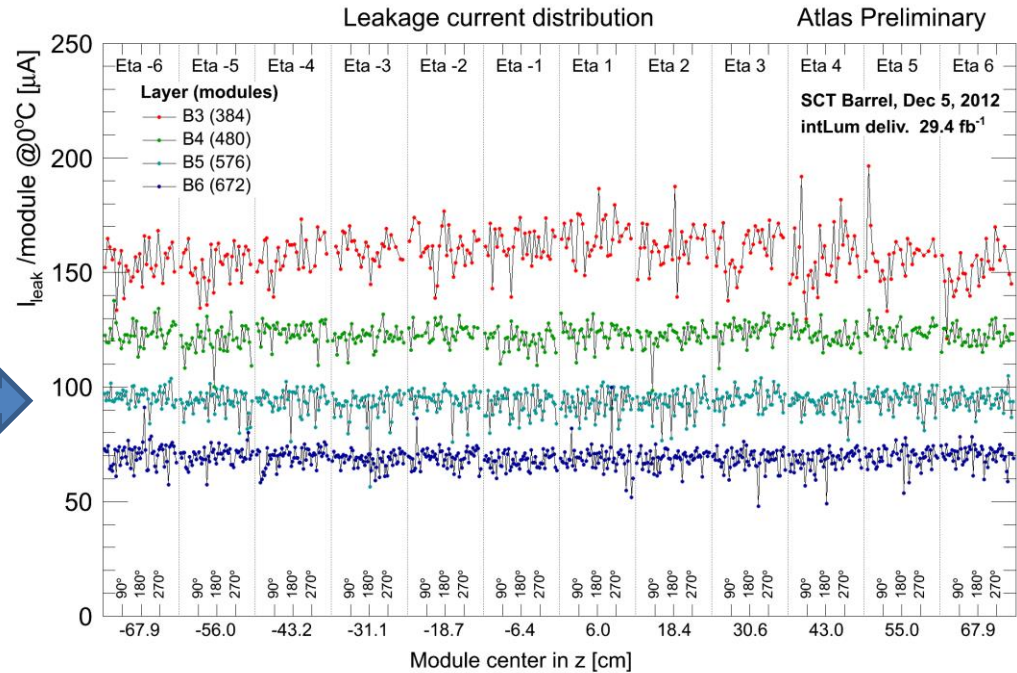


- (1) ENC of <111> modules decreased in 2010 with chip # dependence.
- (2) Middle CiS modules show increase of 10% in ENC in 2012.
- (3) All chip gain decreased in mid 2011.

HV Current : Barrel case, Dec 2012



Raw HV current observed.



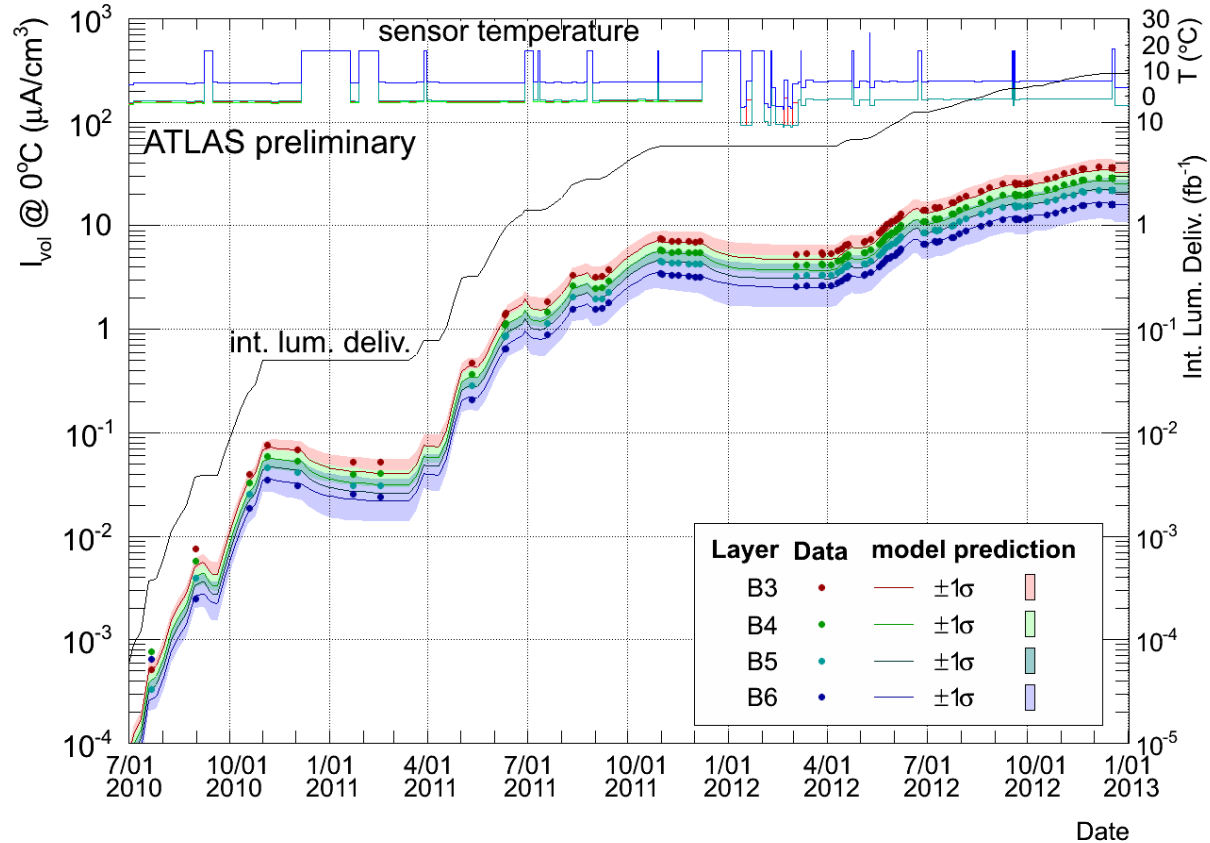
Temperature **corrected** current at 0°C, assuming all are due to the bulk leakage current.

Scaling formula of bulk leakage current:

$$\frac{I(T_{0^\circ\text{C}})}{I(T_{\text{sensor}})} = \left(\frac{T_{0^\circ\text{C}}}{T_{\text{sensor}}} \right)^2 \exp\left(-\frac{E_{\text{gen}}}{2k_B} \left[\frac{1}{T_{0^\circ\text{C}}} - \frac{1}{T_{\text{sensor}}} \right] \right), E_{\text{gen}} = 1.21\text{eV}[1]$$

[1] A.Chilingarov, RD50 Technical Note RD50-2011-01

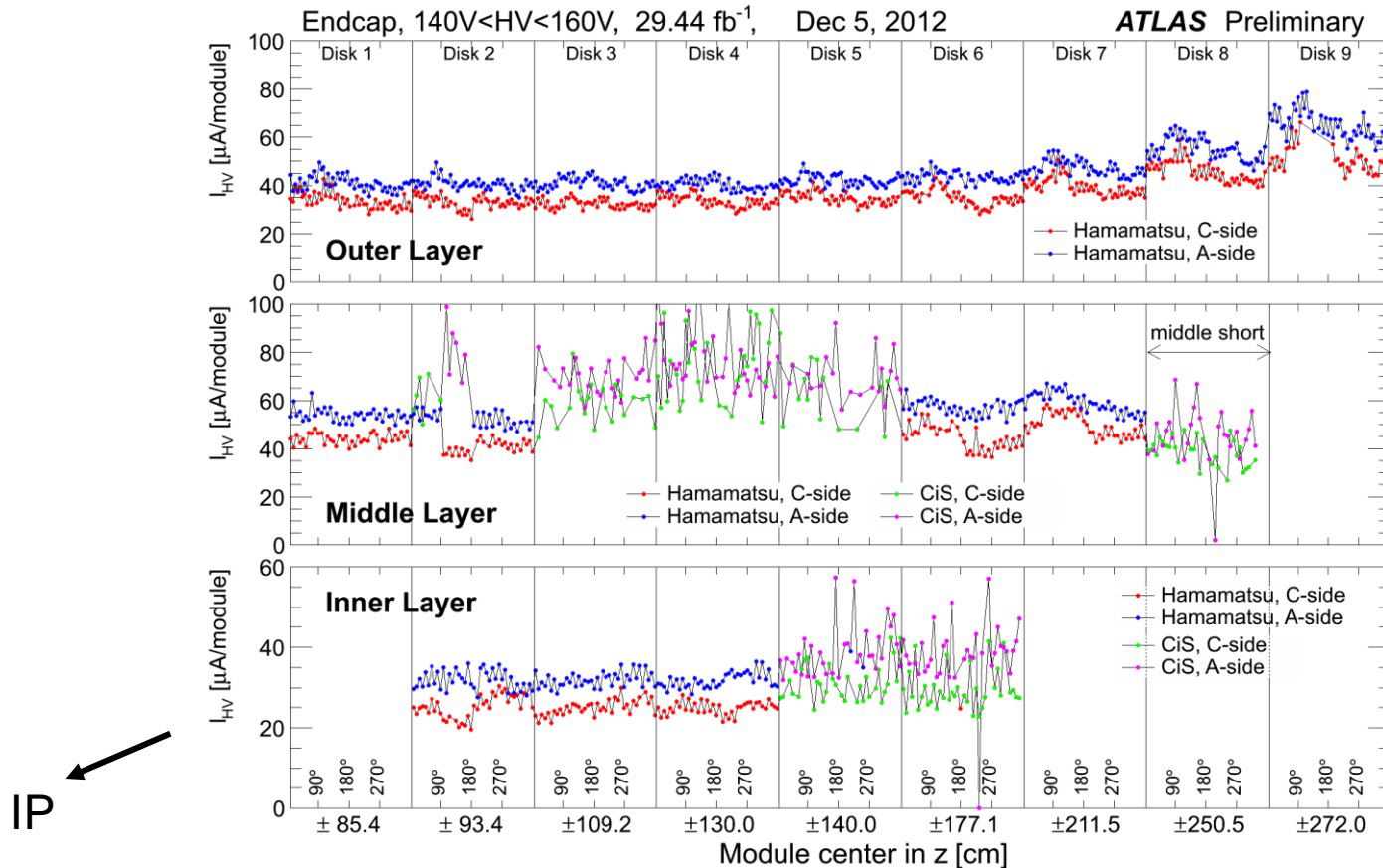
Evolution of leakage current and model prediction



SCT Barrel case

- The data are averaged current at $0^{\circ}C$ of the modules with $HV > 140V$.
- The lines are prediction by the Hamburg/Dortmund model (with no parameter adjustment) including self-annealing effects using sensor temperature history.
- Results of the FLUKA simulation is used to convert the delivered luminosity to 1 MeV neutron-equivalent fluence at corresponding barrel layers.

Raw HV Current : Endcap case, Dec 2012



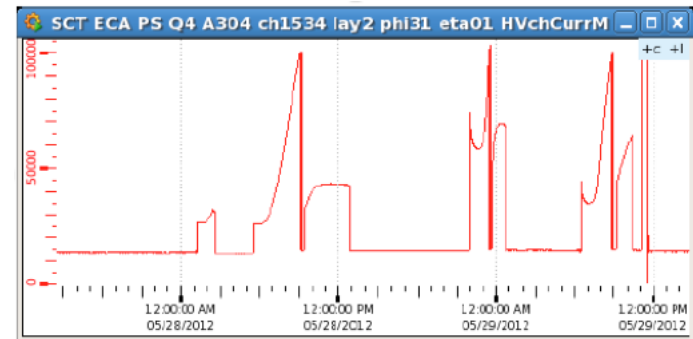
red: side C

blue: side A

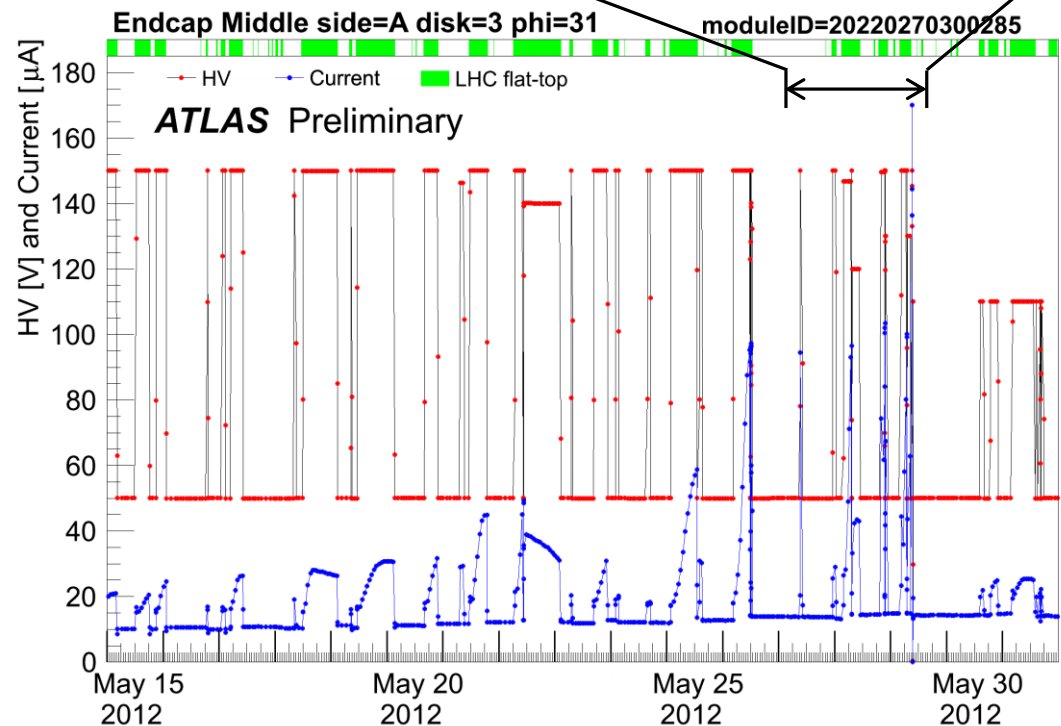
- (1) Modules of side-A systematically show higher current by $\sim 20\%$ probably due to different environment N_2 temperatures.
- (2) Disks 8 and 9 show higher current, similar to the Fluka results.
- (3) We have a difficulty to normalize to 0°C due to large uncertainty in the estimate of the sensor temperature using the hybrid temperature.

Anomalous current in modules with CiS sensors (1)

- At around the end of May 2012, we have experienced unrecoverable ROD busy after a few hours into stable beam only with high luminosity.
- It was due to high current of modules with CiS sensors in middle endcap layers.
- The HV current varies during the beam time.
- Tentative solution : to keep the stand-by voltage at 5V (instead of 50V).
- Some sensors now operate at lower bias voltages, but marginally affecting efficiency.



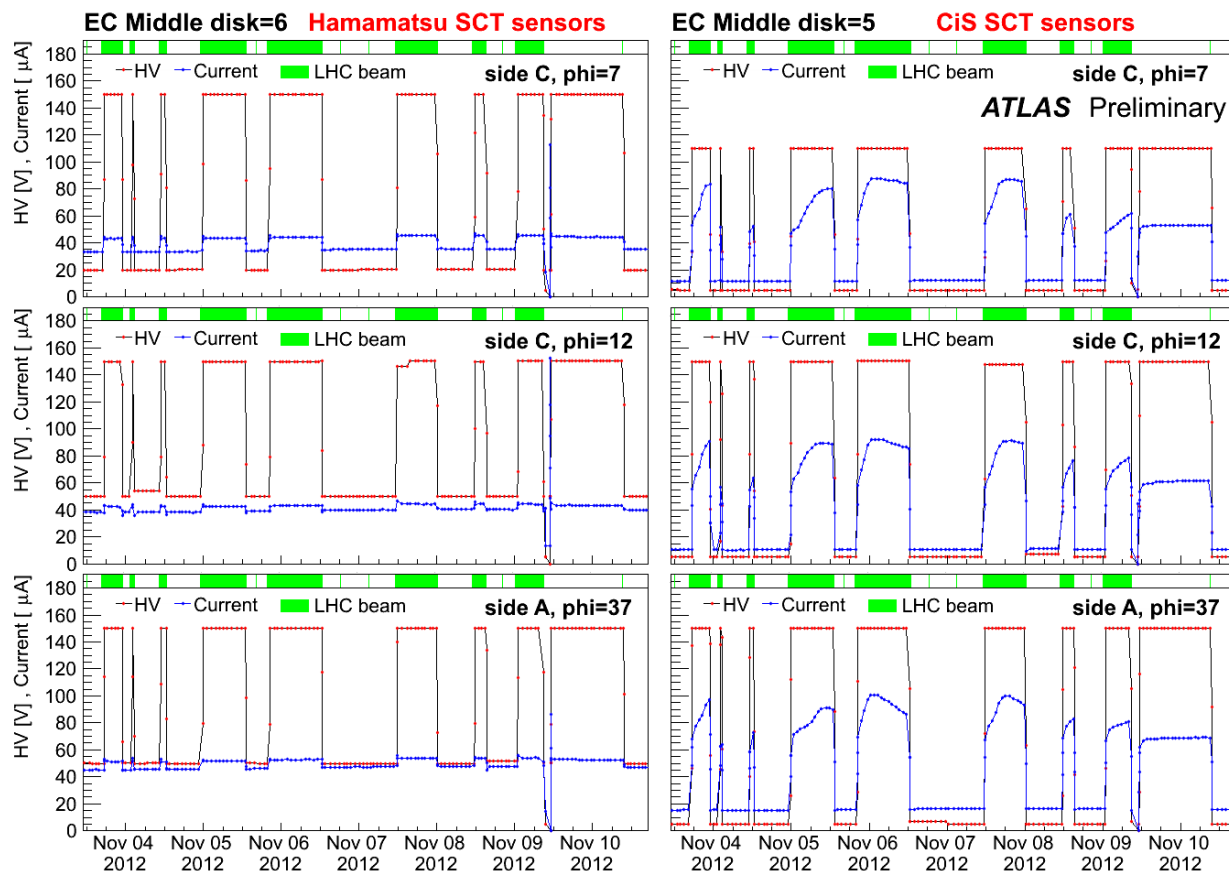
Online display



Example of HV current deterioration

red : Bias Voltage , blue : HV Current


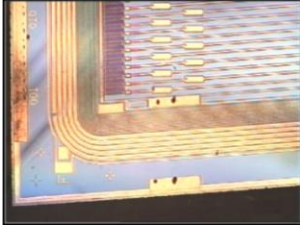
Anomalous current in modules with CiS sensors (2)



- HV/Current profiles in early Nov. 2012 with long stable beam runs.
- Typical 3 modules with **Hamamatsu** (left) **CiS** (right) sensors in close locations from C and A sides.
- The last run is a day-long calibration with no LHC beam.

- (1) All Hamamatsu modules show stable current with/without beams.
- (2) All CiS modules simultaneously (but with different amount) exhibit similar current shapes only during beam time, in both sides A and C. However, the current shape differs run by run. Excess current disappears by turning HV down to stand-by voltage of 5V.

SCT sensors: “same spec, different species” [1]

Points of differences		
Manufacturers	Hamamatsu	CiS
Bias resistors (1.25MΩ)	polysilicon	implant meander
Al strip/implant widths	22/16 μm	16/20 μm
Guard ring	single ring, floating	11+5 p ⁺ rings, potential by punch-through current
Front surface passivation	SiO ₂	SiO ₂ and Si ₃ N ₄
Rear metal HV contact	unpolished	polished
Bulk material	standard	standard (middle) oxygen-enriched (inner)
Micro-discharge	no	a problem at low(<30%) RH

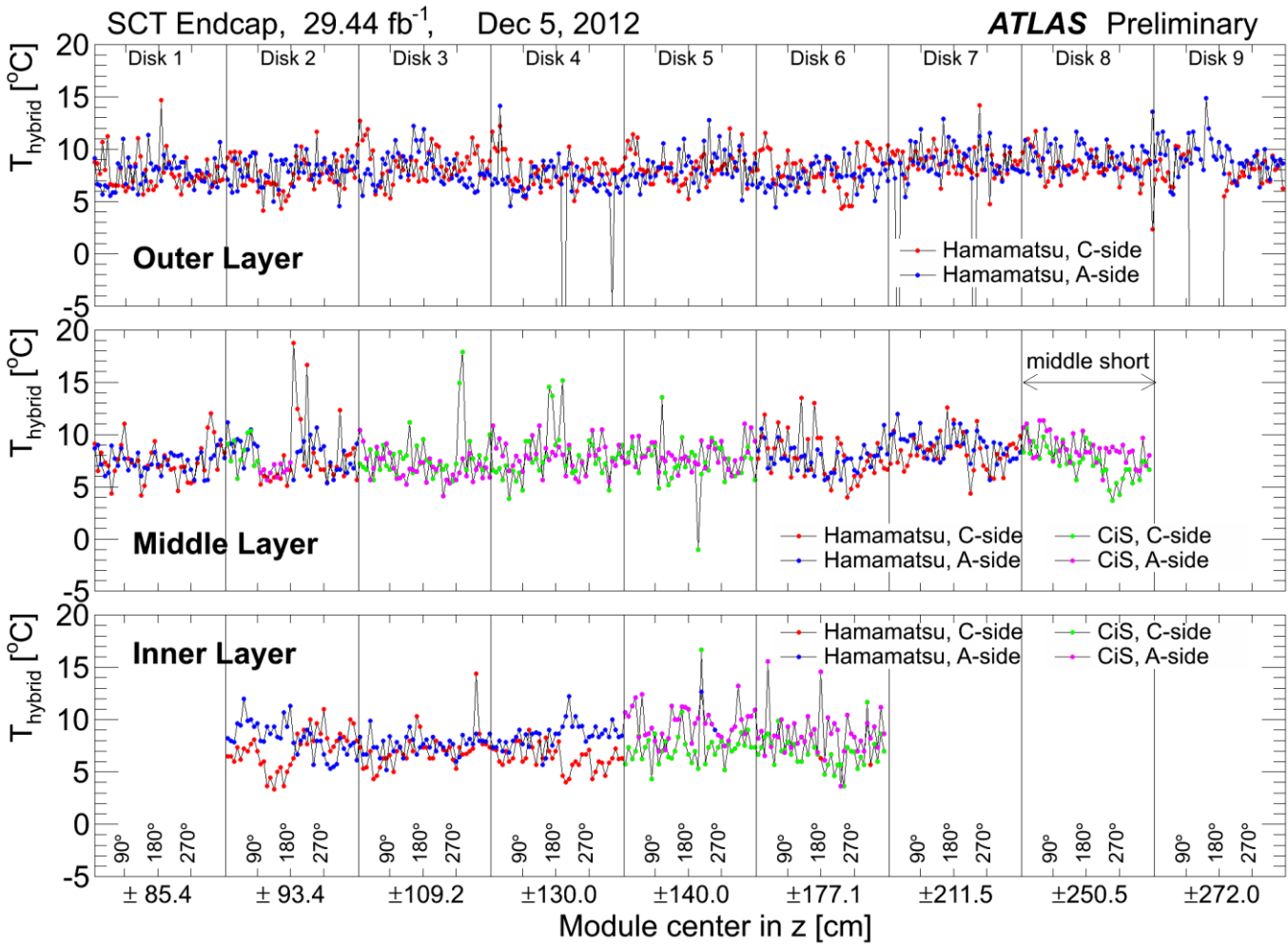
[1] A. Ahmad et al., NIM A NIMA 578 (2007) 98–118.

Summary

- The Barrel layer B3 received $5 \times 10^{12}/\text{cm}^2$ 1MeV n-equivalent fluence by the end of 2012.
- The cooling system has been working very well sustaining the uniform and stable temperatures for all modules.
- The noise (ENC) and gain have been rather stable except for noise of the middle modules with CiS sensors.
- The HV current at 150V steadily increased. Barrel layers show very flat distribution. The model predictions including annealing effects reproduce the leakage current within 1σ ($\sim 20\%$) with no parameter re-adjustments.
- All modules with CiS sensors are showing simultaneously anomalous current only during the beam times. No such anomalies are seen in any of modules with Hamamatsu sensors.

Backup slides

Endcap hybrid Temperature on Dec 2012: each module

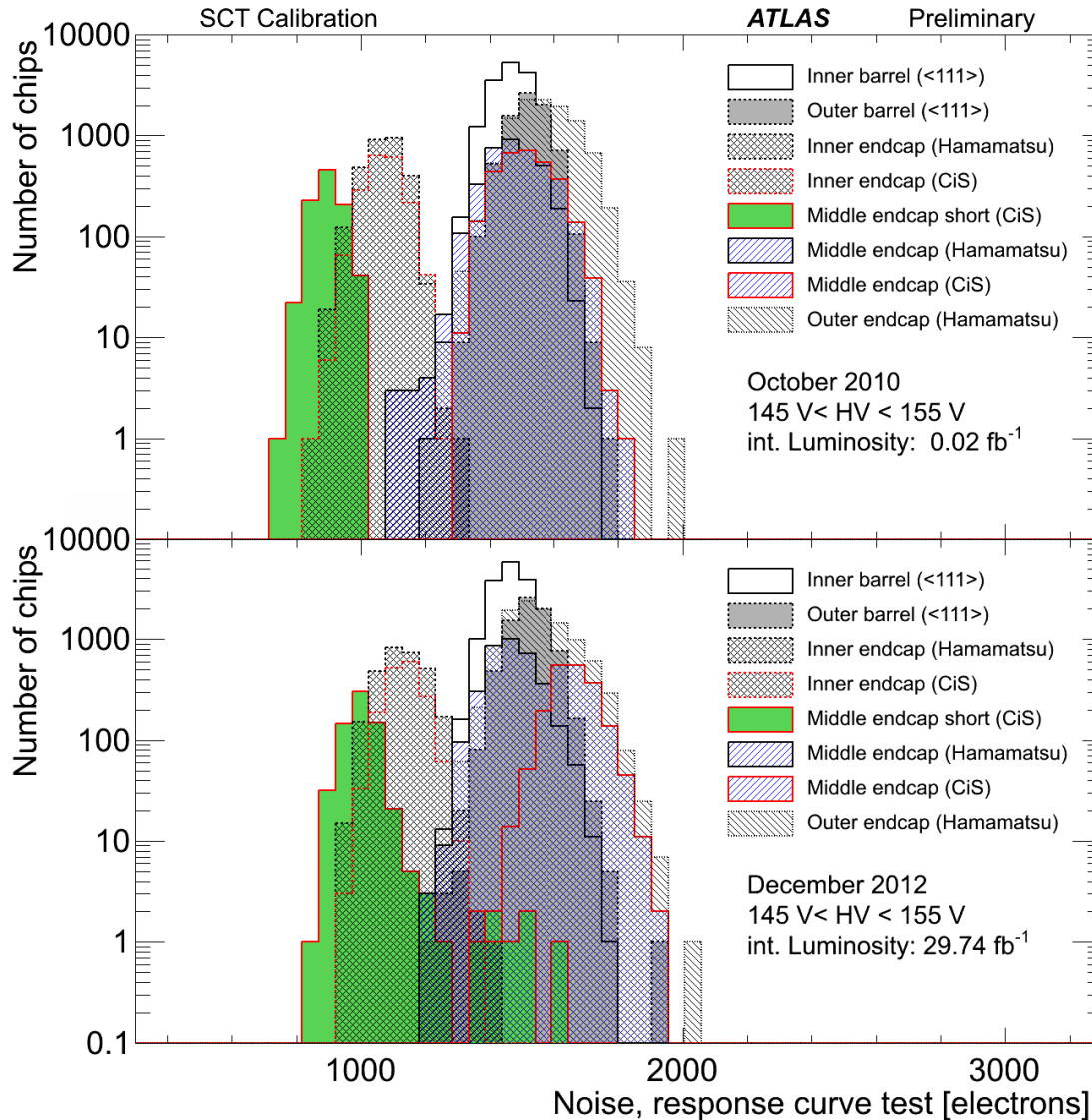


Hamamatsu
 red: C-side
 blue: A-side

CiS
 green: C-side
 pink: A-side

← Note special x axis values

Noise chip by chip in log scale

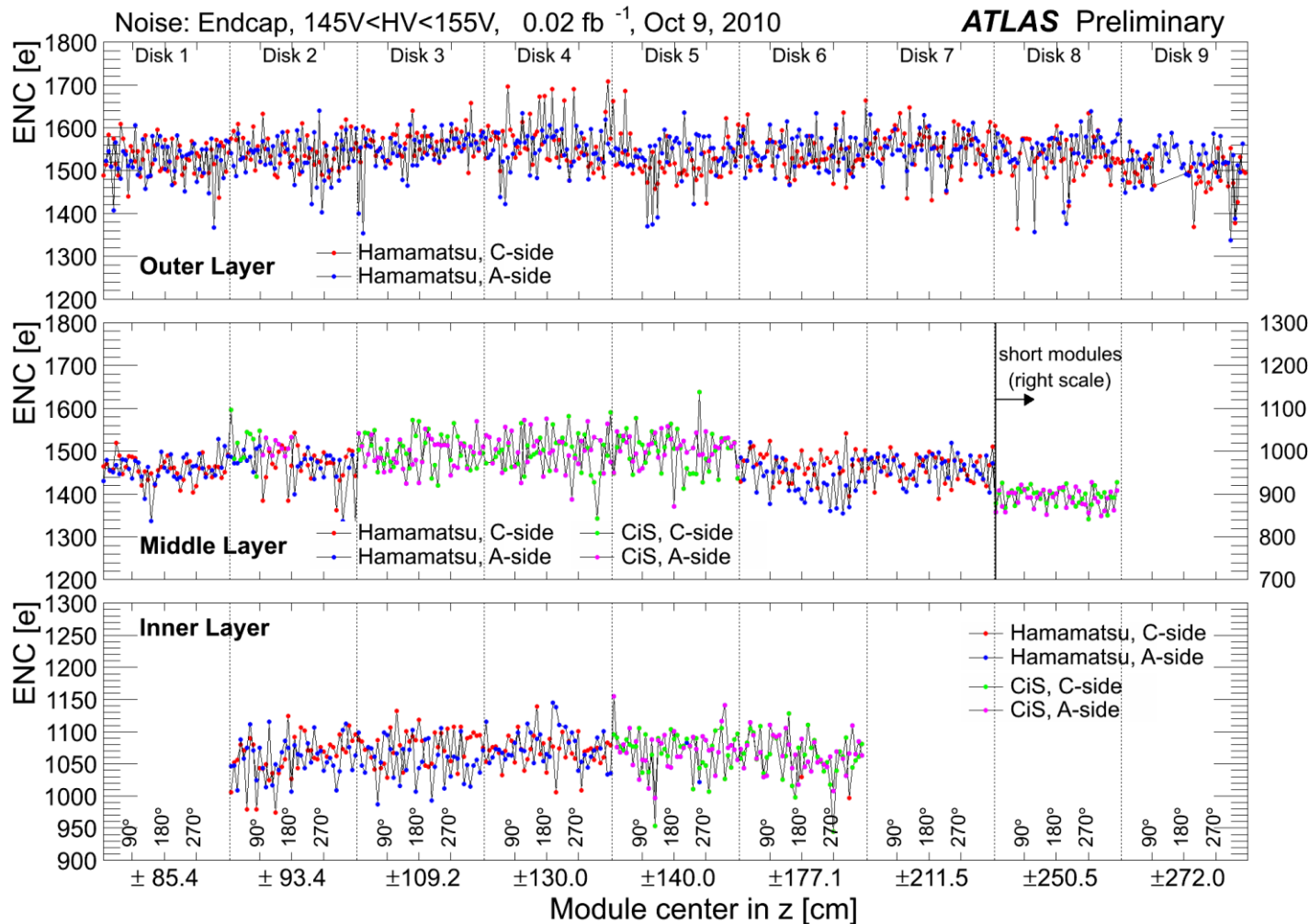


Oct. 2010

Dec. 2012

No wide tails.

Noise : Endcap, Oct 2010, near the start-up

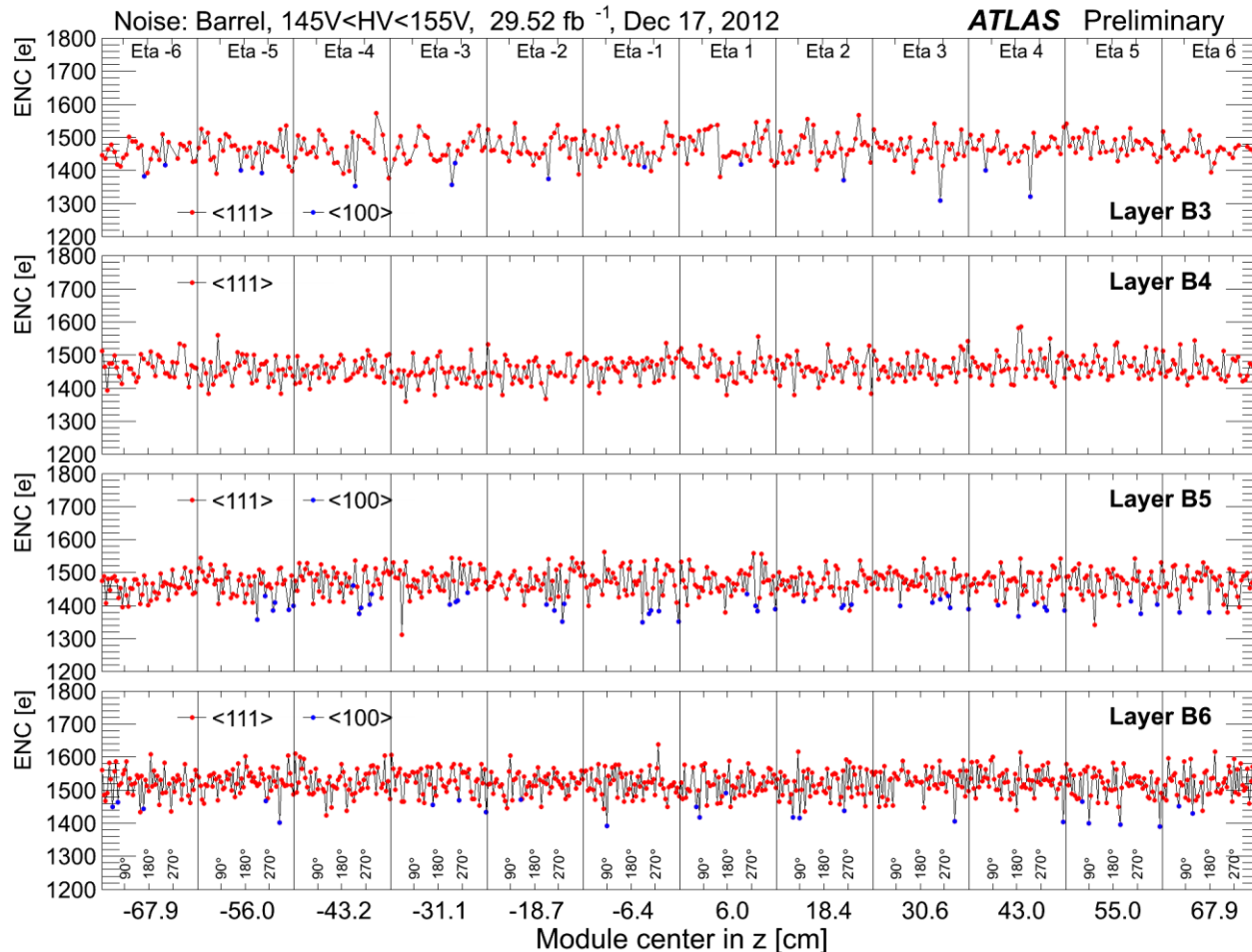


Hamamatsu
red: C-side
blue: A-side

CiS
green: C-side
pink: A-side

Noises of CiS modules were comparable with those of Hamamatsu modules in 2010.

Noise : Barrel, Dec 2012



Hamamatsu
red: <111>
blue: <100>

- (1) Noise is very uniform over entire Barrel area.
- (2) Noise of all <100> modules is lower than those of <111> modules.

Hamburg/Dortmund model for bulk leakage current

Based on Moll's thesis [1], the leakage current coefficient a is given by Krasel [2] is

$$\alpha(t) = \alpha_I \cdot \exp\left(-\frac{t}{\tau_I}\right) + \alpha_0^* - \beta \cdot \ln(\Theta(T_a)t/t_0)$$

$$\alpha_I = (1.23 \pm 0.06) \cdot 10^{-17} \text{ A/cm}$$

$$\frac{1}{\tau_I} = k_{0I} \cdot \exp\left(-\frac{E_I}{k_B T_a}\right), \quad t_0 = 1 \text{ min.}$$

$$k_{0I} = 1.2_{-1.0}^{+5.3} \cdot 10^{13} \text{ s}^{-1}, \quad E_I = (1.11 \pm 0.05) \text{ eV}$$

$$\Theta(T_a) = \exp\left[-\frac{E_I^*}{k_B} \left(\frac{1}{T_a} - \frac{1}{T_{ref}}\right)\right]$$

$$\alpha_0^* = 7.07 \cdot 10^{-17} \text{ A/cm}$$

$$\beta = 3.29 \cdot 10^{-18} \text{ A/cm}$$

$$E_I^* = (1.30 \pm 0.14) \text{ eV}$$

$$T_{ref} = 21^\circ\text{C}$$

$$G_i = G_i^{\text{exp}} + G_i^{\text{log}}$$

$$G_i^{\text{exp}} = \sum_{j=1}^i \Phi_{eq,j} \alpha_I \exp\left(-t_{i,j}^I / \tau_I(20^\circ\text{C})\right)$$

$$t_{i,j}^I = \sum_{j=1}^i \Delta t_j \cdot \frac{\tau_I(20^\circ\text{C})}{\tau_I(T_j)}$$

$$G_i^{\text{log}} = \sum_{j=1}^i \Phi_{eq,j} \left(\alpha_0^* - \beta \cdot \ln(t_{i,j}^{\text{log}} / t_0)\right)$$

$$t_{i,j}^{\text{log}} = \sum_{k=j}^i \Delta t_k \cdot \Theta(T_k)$$



Note : last two equations in [2] are corrected here.

[1] M. Moll, DESY-THESIS-1999-040 (Dec 1999)

[2] Oraf Krasel, Dortmund Dissertation, July 2004

SCT: recent talks and publications

2010.8	Vertex2010	U. Bitenc	Atlas Silicon Strips Operations and Performance
2010.11	ATL-INDET-PROC-2010-036	P. Haefner	The ATLAS SCT Operation and Performance
2011.5	ATL-COM-INDET-2011-001	I. Dawson et al.	Fluence and dose measurements in the ATLAS inner detector and comparison with simulation
2011.	ATL-COM-INDET-2011-013	Y. Pylypchenko	Operation and Performance of ATLAS SCT
2011.11	Workshop on Quality Issues in Current and Future Silicon Detectors		
		D. Robinson	Sensor Quality Assurance for ATLAS SCT
2011.12	HSTD8	D. Robinson	ATLAS SCT Operation and Performance
2012.2	7 th Trent workshop	P. Johansson	ATLAS SCT Operation and Performance
2012.5	RD20 workshop	T. Kondo	Status of radiation damage of the ATLAS SCT detector
2012.9	Vertex2012	S. Yacoob	Operational issues of present ATLAS strip detector
2012.9	Vertex2012	I. Dawson	Radiation Background Simulation and Verification at the LHC and Its Upgrades
2012.10	IEEE NSS2012	S. D'Auria	ATLAS SCT Operation and Performance